



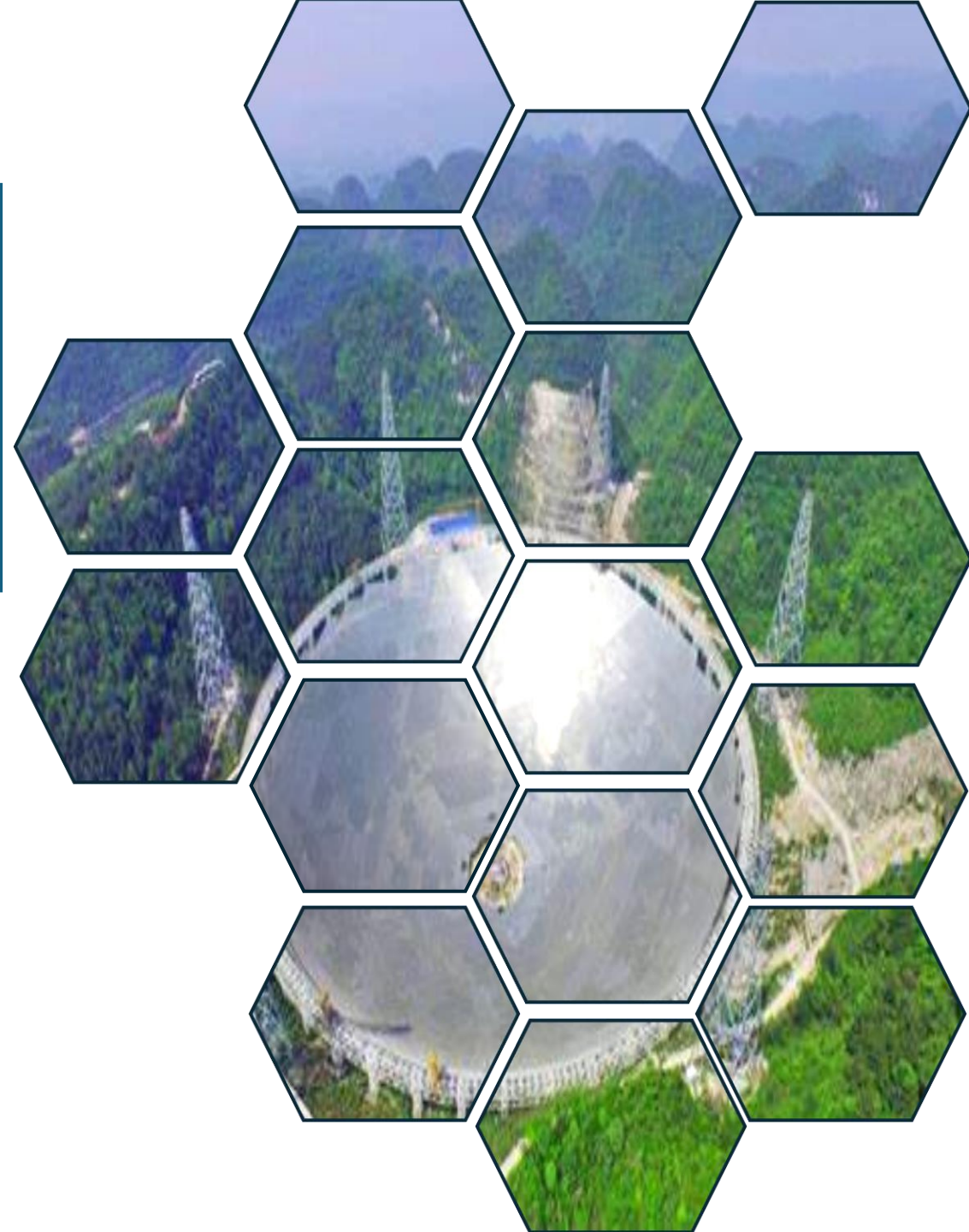
Probing Large-Scale Structure with HI-SZ Cross-Correlation

Ayodeji Ibitoye

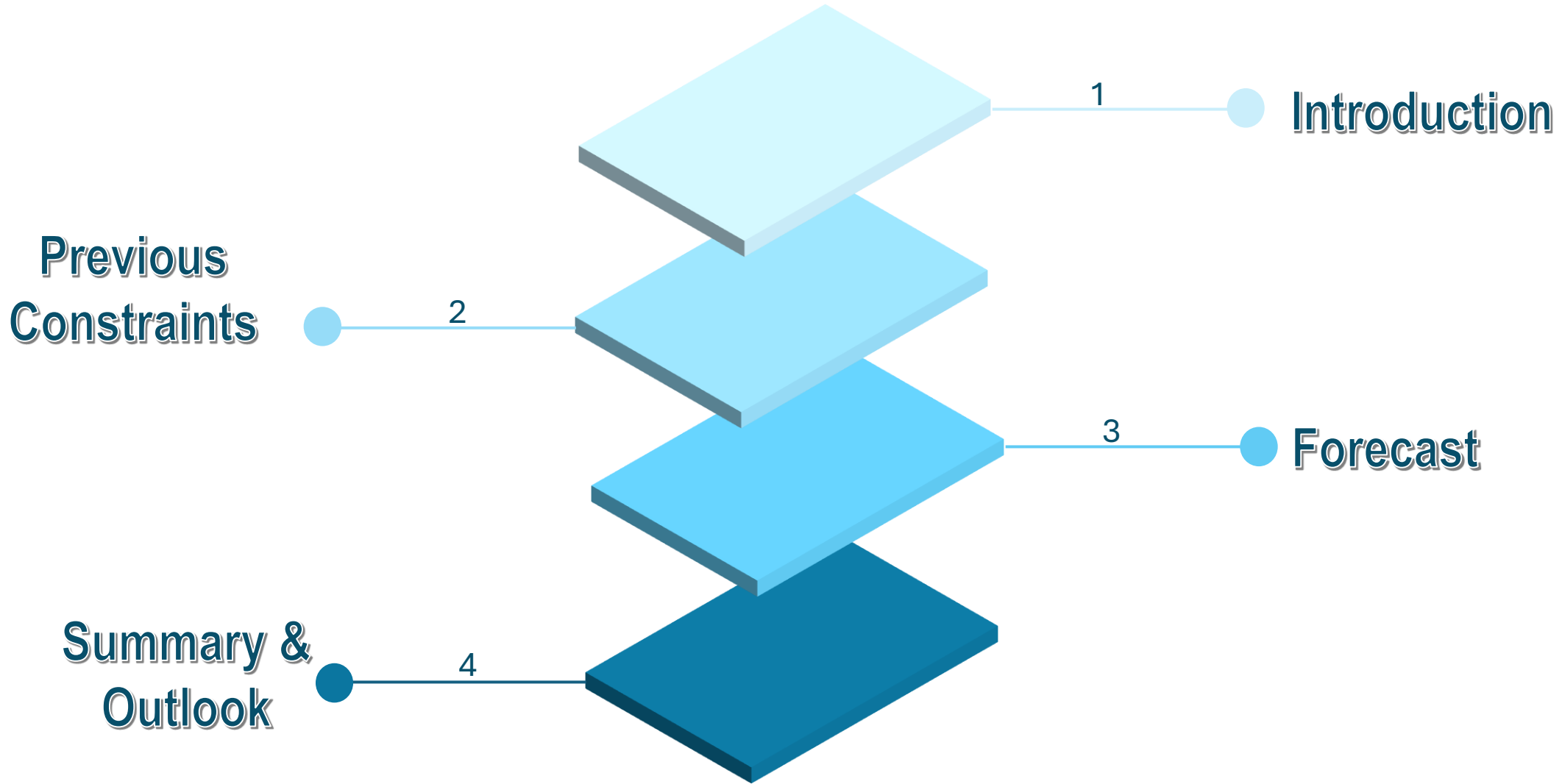
(Collaboration with Furen Deng, Yichao Li, YinZhe Ma,
Gong Yan, Xuelei Chen)

Dark Matter and Dark Energy Research group, NAOC-CAS, Beijing.

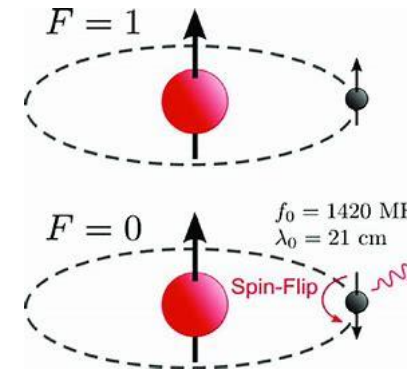
21cm Cosmology Workshop 2024
& Tianlai Collaboration Meeting
Tuesday, 23rd July, 2024



OUTLINE



21cm line as a cosmological probe



- 21 cm (1.4 GHz) line becoming a versatile probe in cosmology
- Hydrogen abundance, not much confusion from other lines
- A “forbidden” transition, ~ 10 Myr lifetime of excited state \Rightarrow observed frequency gives a good measurement of the redshift of emission.
- $1 + z = \frac{1420}{\nu_{obs}}$
- Sensitive to study the history of matter and growth of structure in the Universe.

Current Observations



SZ effect

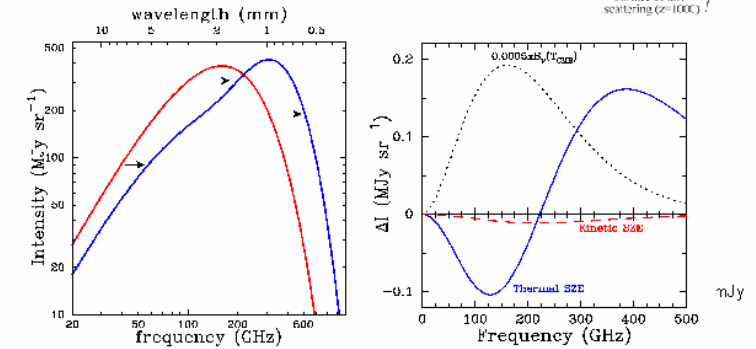
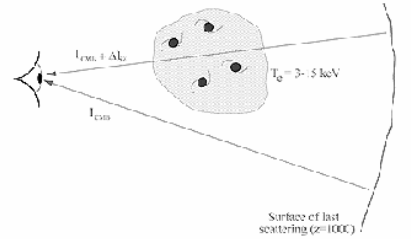
Thermal SZ

Kinetic SZ

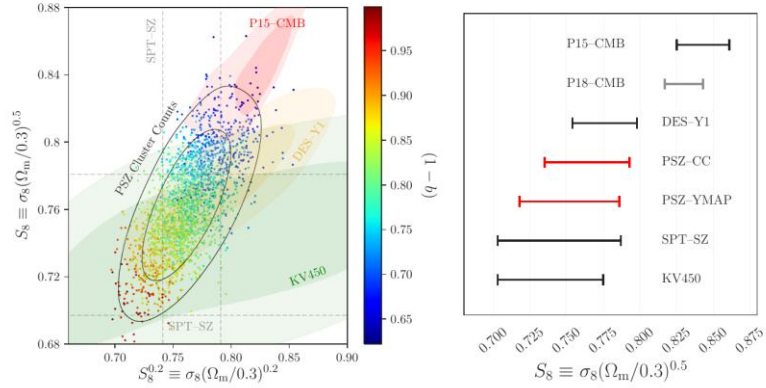
Polarized SZ

Sunyaev-Zel'dovich Effect

$$\frac{\Delta T}{T_{\text{CMB}}} = g(x) \int dl n_e(l) \frac{k_B T_e(l)}{m_e c^2} \sigma_T$$



The tSZ probe



THE ASTROPHYSICAL JOURNAL SUPPLEMENT SERIES, 270:16 (19pp), 2024 January
 © 2024. The Authors. Published by the American Astronomical Society.

<https://doi.org/10.3847/1538-4365/ad88c5>

OPEN ACCESS



Cross Correlation between the Thermal Sunyaev-Zeldovich Effect and the Integrated Sachs-Wolfe Effect

Ayodeji Ibitoye^{1,2}, Wei-Ming Dai³, Yin-Zhe Ma^{1,2,3}, Patricio Vielva⁴, Denis Tramontè⁵, Amare Abebe^{5,8}, Aroonkumar Beesham^{5,9,10}, and Xuefei Chen¹

¹ National Astronomical Observatories, Chinese Academy of Sciences, 20A Datun Road, Chaoyang District, Beijing 100101, People's Republic of China

² Department of Physics and Electronics, Adekunle Ajasin University, P. M. B. 001, Akungba-Akoko, Ondo State, Nigeria

³ School of Physical Science and Technology, Ningbo University, Ningbo 315211, People's Republic of China

⁴ Department of Physics, Stellenbosch University, Matieland, Western Cape, 7602, South Africa; muyinze@sun.ac.za

⁵ National Institute for Theoretical and Computational Sciences (NITheCS), 7602, South Africa

⁶ Instituto de Física de Cantabria (CSIC-UC), Avda. Los Castros s/n, E-39005 Santander, Spain

⁷ Department of Physics, Xi'an Jiaotong-Liverpool University, 111 Ren'ai Road, Suzhou Dushu Lake Science and Education Innovation District, Suzhou Industrial Park, Suzhou 215123, People's Republic of China

⁸ Centre for Space Research, North-West University, Potchefstroom 2520, South Africa

⁹ Department of Mathematical Sciences, University of Zululand, Private Bag X1001, Kwa-Dlangezwa 3886, South Africa

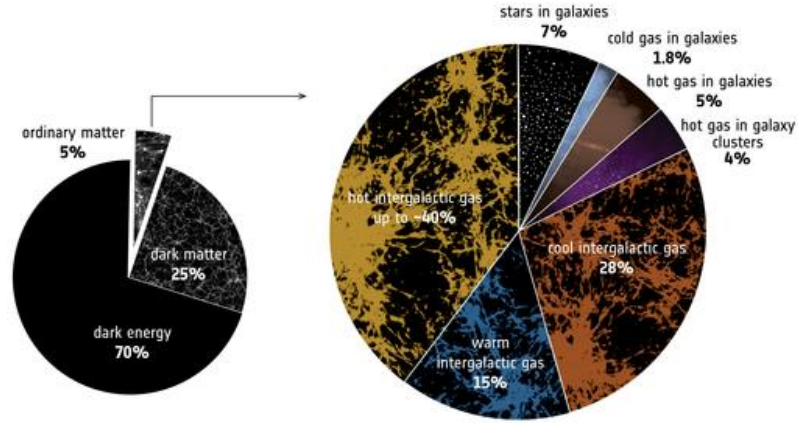
¹⁰ Faculty of Natural Sciences, Mangosuthu University of Technology, P.O. Box 12363, Jacobs 4052, South Africa

Received 2023 May 19; revised 2023 October 12; accepted 2023 October 27; published 2024 January 12

Abstract

We present a joint cosmological analysis of the power spectra measurement of the Planck Compton parameter and the integrated Sachs-Wolfe (ISW) maps. We detect the statistical correlation between the Planck thermal Sunyaev-Zeldovich (tSZ) map and ISW data with a significance of a **3.6 σ confidence level (CL)**, with the autocorrelation of the Planck tSZ data being measured at a 25 σ CL. The joint auto- and cross-power spectra constrain the matter density to be $\Omega_m = 0.317^{+0.009}_{-0.011}$, the Hubble constant to be $H_0 = 66.5^{+2.0}_{-2.0}$ km s⁻¹ Mpc⁻¹, and the rms matter density fluctuations to be $\sigma_8 = 0.730^{+0.040}_{-0.040}$ at the 68% CL. The derived large-scale structure S_8 parameter is $S_8 \equiv \sigma_8(\Omega_m/0.3)^{0.5} = 0.755 \pm 0.060$. If using only the diagonal blocks of covariance matrices, the Hubble constant becomes $H_0 = 69.7^{+2.0}_{-2.0}$ km s⁻¹ Mpc⁻¹. In addition, we obtain the constraint of the product of the gas bias, gas temperature, and density as $b_{\text{gas}}(T_e/(0.1 \text{ keV}))(\bar{n}_e/1 \text{ m}^{-3}) = 3.09^{+0.320}_{-0.320}$. We find that this constraint leads to an estimate on the electron temperature today as $T_e = (2.40^{+0.20}_{-0.20}) \times 10^6$ K, consistent with the expected temperature of the warm-hot intergalactic medium. Our studies show that the ISW-tSZ cross correlation is capable of probing the properties of the large-scale diffuse gas.

Unified Astronomy Thesaurus concepts: Large-scale structure of the universe (902)



OPEN ACCESS



Cross Correlation between the Thermal Sunyaev-Zel'dovich Effect and Projected Galaxy Density Field

Ayodeji Ibitoye^{1,2,3}, Denis Tramontè^{1,2,4}, Yin-Zhe Ma^{1,2,4}, and Wei-Ming Dai^{1,2}

¹ School of Chemistry and Physics, University of KwaZulu-Natal, Westville Campus Private Bag X54001, Durban, 4000, South Africa; ma@ukzn.ac.za

² NAOC-UKZN Computational Astrophysics Centre (NUCAC) University of KwaZulu-Natal, Durban, 4000, South Africa

³ Department of Physics and Electronics, Adekunle Ajasin University P.M. B. 001, Akungba-Akoko, Ondo State, Nigeria

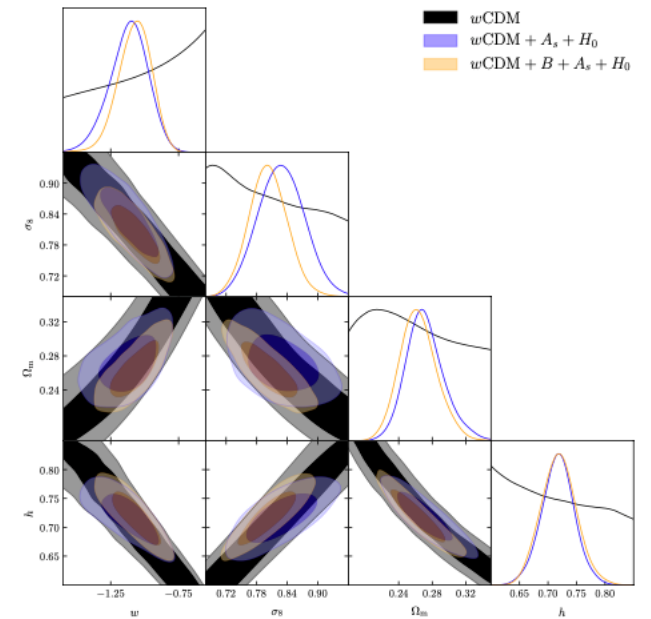
⁴ Purple Mountain Observatory, CAS, No.10 Yuanhua Road Qixia District, Nanjing 210034, People's Republic of China

Received 2021 November 10; revised 2022 May 31; accepted 2022 June 11; published 2022 August 9

Abstract

We present a joint analysis of the power spectra of the Planck Compton y parameter map and the projected galaxy density field using the Wide Field Infrared Survey Explorer (WISE) all-sky survey. We detect the statistical correlation between WISE and Planck data (gy) with a significance of **21.8 σ** . We also measure the autocorrelation spectrum for the thermal Sunyaev-Zel'dovich (tSZ) (yy) and the galaxy density field maps (gg) with a significance of **150 σ** and **88 σ** , respectively. We then construct a halo model and use the measured correlations C_l^{yy} , C_l^{gy} , and C_l^{gg} to constrain the tSZ mass bias $B \equiv M_{500}/M_{500}^{\text{SZ}}$. We also fit for the galaxy bias, which is included with explicit redshift and multipole dependencies as $b_g(z, \ell) = b_g^0(1+z)^{\beta_g}(\ell/\ell_0)^{\alpha_g}$, with $\ell_0 = 117$. We obtain the constraints to be $B = 1.50 \pm 0.07(\text{stat}) \pm 0.34(\text{sys})$, i.e., $1 - b_{\text{H1}} = 0.67 \pm 0.03(\text{stat}) \pm 0.16(\text{sys})$ (68% confidence level) for the hydrostatic mass bias, and $b_g^0 = 1.28^{+0.03}_{-0.04}(\text{stat}) \pm 0.11(\text{sys})$, with $\alpha = 0.20^{+0.11}_{-0.11}(\text{stat}) \pm 0.10(\text{sys})$ and $\beta = 0.45 \pm 0.01(\text{stat}) \pm 0.02(\text{sys})$ for the galaxy bias. Incoming data sets from future CMB and galaxy surveys (e.g., Rubin Observatory) will allow probing the large-scale gas distribution in more detail.

Unified Astronomy Thesaurus concepts: Sunyaev-Zeldovich effect (1654); Infrared galaxies (790)

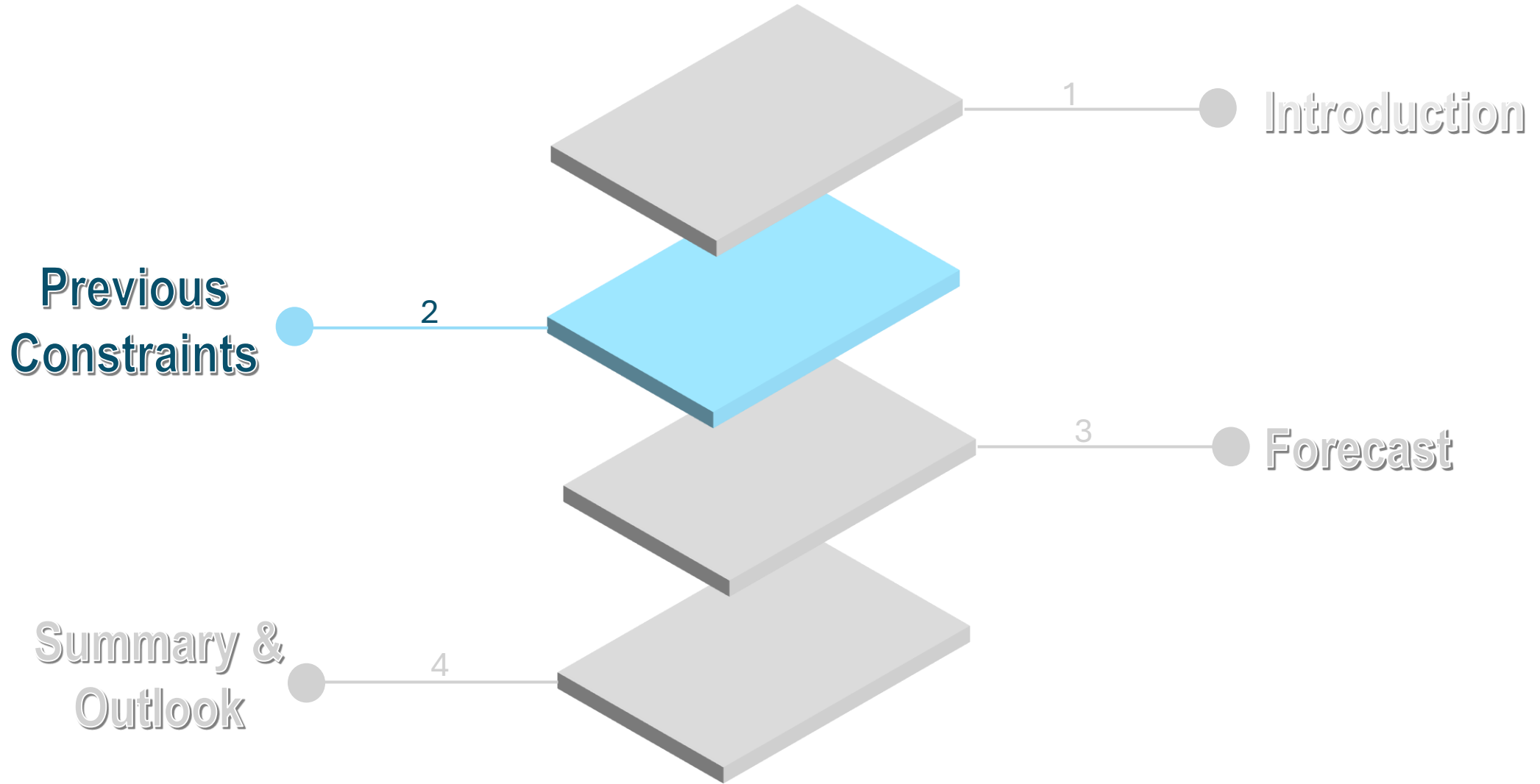


■ Ibitoye et. al. 2024

■ Ibitoye et. al. 2022

■ Bolliet et. al. 2018

OUTLINE



Constraining power of 21 cm related studies



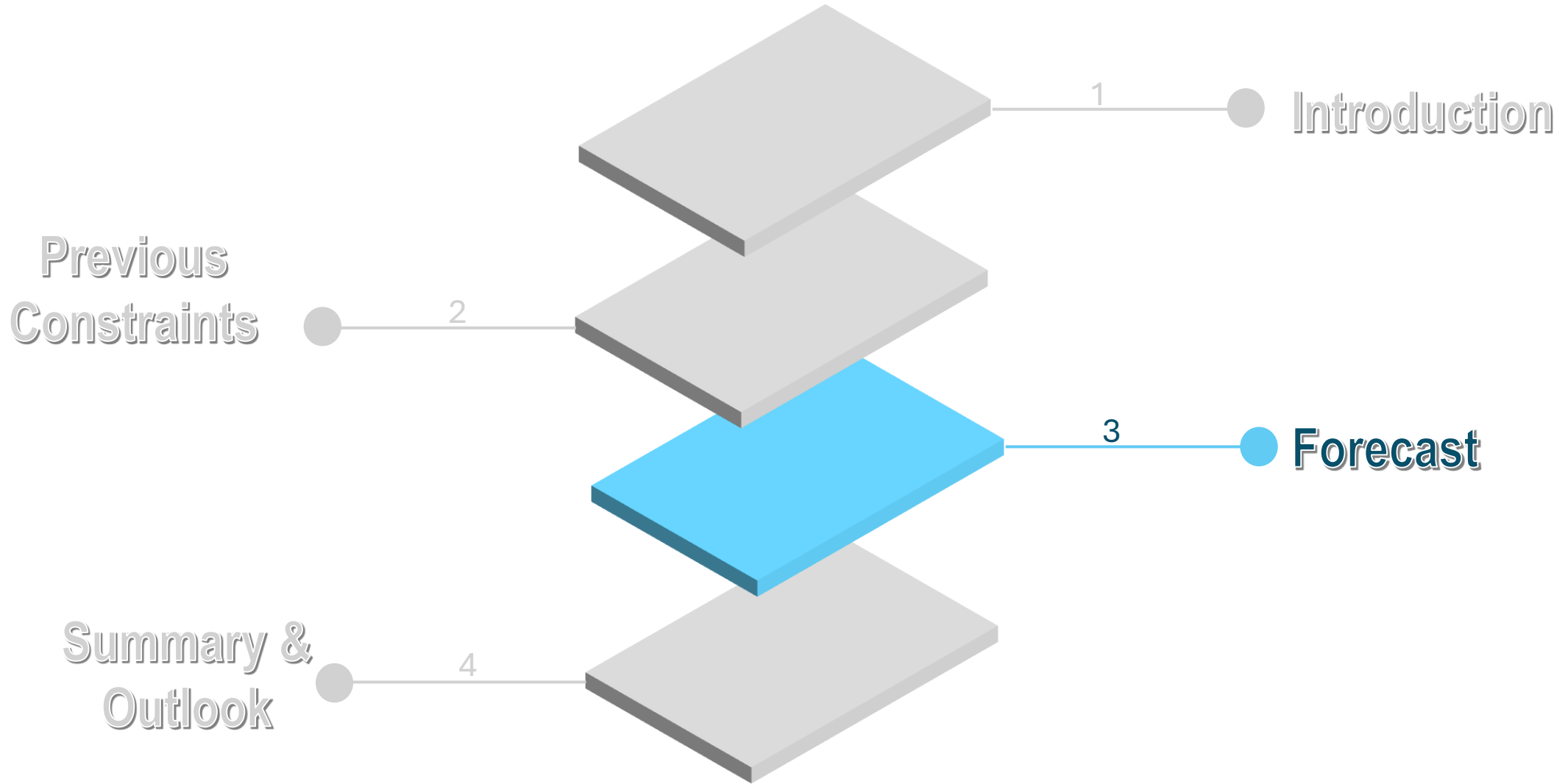
Technique	Constraints (Ω_{HI} are $h^{-1} \times 10^{-4}$)	Mean redshift (Redshift range)	Reference
Galaxy surveys			
ALFALFA HI emission	$\Omega_{\text{HI}}^* = 3.0 \pm 0.2$	0.026	Martin et al. (2010)
HIPASS HI emission	$\Omega_{\text{HI}} = 2.6 \pm 0.3$	0.015	Zwaan et al. (2005)
HIPASS, Parkes; HI stacking	$\Omega_{\text{HI}} = 2.82^{+0.30}_{-0.59}$	0.028 (0 - 0.04)	Delhaize et al. (2013)
	$\Omega_{\text{HI}} = 3.19^{+0.43}_{-0.59}$	0.096 (0.04 - 0.13)	
AUDS HI emission from galaxies + HI surveys + stacking	$\Omega_{\text{HI}} = 2.63 \pm 0.1$	0.065 (0.0 - 0.2)	Hoppmann et al. (2015)
GMRT HI emission stacking	$\Omega_{\text{HI}} = (5.0 \pm 1.8)h$	0.32	Rhee et al. (2018)
uGMRT HI emission stacking	$\Omega_{\text{HI}} = (4.81 \pm 0.75)h$	$0.2 < z < 0.4$	Bera et al. (2019)
uGMRT HI stacking, DEEP2 field	$\Omega_{\text{HI}} = (4.5 \pm 1.1)h$	~ 1.06	Chowdhury et al. (2020)
MIGHTEE-HI: first MeerKAT HI mass function	$\Omega_{\text{HI}} = 5.46^{+0.94}_{-0.99}$	$0 \leq z \leq 0.084$	Ponomareva et al. (2023)
MIGHTEE-HI: first MeerKAT HI mass function obtained using Modified Maximum Likelihood (MML)	$\Omega_{\text{HI}} = 6.31 \pm 0.31$	$0 \leq z \leq 0.084$	Ponomareva et al. (2023)
HI distribution maps from M31, M33 and LMC	$\Omega_{\text{HI}} = 3.83 \pm 0.64$	0.0	Braun (2012)
DLA observations			
DLA measurements from HST and SDSS	$\Omega_{\text{HI}} = 5.2 \pm 1.9$	0.609 (0.11 - 0.90)	Rao et al. (2006)
	$\Omega_{\text{HI}} = 5.1 \pm 1.5$	1.219 (0.90 - 1.65)	
	$\Omega_{\text{HI}} = 4.29^{+0.24}_{-0.23}$	(2.2 - 5.5)	
	$\Omega_{\text{HI}}(z)$	(2.0 - 5.19)	
Cross-correlation of DLA and Ly- α forest observations	$b_{\text{DLA}} = 2.17 \pm 0.2$	~ 2.3	Font-Ribera et al. (2012)
Observations of DLAs with HST/COS	$\Omega_{\text{HI}} = 9.8^{+9.1}_{-4.9}$	< 0.35	Meiring et al. (2011)
DLAs and sub-DLAs with VLT/UVES	$\Omega_{\text{HI}}(z)$	1.5 - 5.0	Zafar et al. (2013)

Constraining power of 21 cm related studies

	HI intensity mapping		
WSRT HI emission	$\Omega_{\text{HI}} = 2.22 \pm 0.40$	0.1	
	$\Omega_{\text{HI}} = 2.29 \pm 0.61$	0.2	Rhee et al. (2013)
DINGO HI emission	$\Omega_{\text{HI}} = 4.20 \pm 0.8$	0.057	
	$\Omega_{\text{HI}} = 4.60 \pm 0.7$	0.008	Rhee et al. (2023)
Cross-correlation of DEEP2 galaxy-HI fields	$\Omega_{\text{HI}} b_{\text{HI}} r^\dagger = (5.5 \pm 1.5)h$	0.8	Chang et al. (2010)
HI intensity fluctuation	$\Omega_{\text{HI}} b_{\text{HI}} r = (4.3 \pm 1.1)h$	0.8	Masui et al. (2013)
cross-correlation with WiggleZ survey			
MeerKAT HI IM pilot survey	$\Omega_{\text{HI}} b_{\text{HI}} r = (8.6 \pm 1.0 (\text{stat}) \pm 1.2 (\text{sys}))$	0.4 – 0.459	Cunnington et al. (2023)
cross-correlation with WiggleZ survey			
HI auto-power spectrum combined with cross-correlation with WiggleZ survey	$\Omega_{\text{HI}} b_{\text{HI}} = 6.2^{+2.3}_{-1.5}h$	0.8	Switzer et al. (2013)
	Theory/Simulation		
FAST HI Cross-correlation forecast with tSZ	$\sigma(\Omega_{\text{HI}}) = ???$	0 – 0.35	This work
The HI from BINGO project combined with Planck	$\Omega_{\text{HI}} = (6.2 \pm 4.1)h$	0.127 – 0.449	Costa et al. (2022)
Hydrodynamical simulation using GADGET-2/OWLS	$\Omega_{\text{HI}} = (1.4 \pm 0.18)h$	0	
	$\Omega_{\text{HI}} = (2.5 \pm 0.14)h$	1	Duffy et al. (2012a)
	$\Omega_{\text{HI}} = (3.8 \pm 0.08)h$	2	
Galaxy formation simulation, HI astrophysics, based on SKA-MDB2 Survey and SKA-DB1 Survey	$\Omega_{\text{HI}} = 4.3 \pm 0.3$	~ 0.1	
	$\Omega_{\text{HI}} = 4.60 \pm 1.0$	~ 1.0	Chen et al. (2021)
N-body simulation, HI prescription combined with Chang et al. (2010)	$\Omega_{\text{HI}} = (11.2 \pm 3.0)h$	~ 0.8	Khandai et al. (2011)

† r denotes the stochasticity.

OUTLINE



The Halo Model

**HI distributed within
each dark matter halo
(density profile)**
(Padmanabhan et al.
2016, 2017)

**HI distribution of
galaxies within the halo
(HOD)**
(Zheng et al. 2005, Wolz
et.al 2019)

The Halo model

$$\rho_{\text{HI}}(r; M, z) = \rho_0 \exp \left[-\frac{r}{r_s(M, z)} \right] \quad (\text{Density Profile})$$

$$\begin{aligned} \bar{y}_\ell(M_{500}, z) &= \frac{4\pi R_{500}}{\ell_{500}^2} \frac{\sigma_T}{m_e c^2} \quad (\text{2D tSZ field}) \\ &\times \int dx x^2 \frac{\sin(\ell x / \ell_{500})}{\ell x / \ell_{500}} P_e(x; M_{500}, z) \end{aligned}$$

$$\bar{T}_b(z) \frac{W_{\text{HI}}(\chi)}{\chi^2(z)} \frac{M_{\text{HI}}(M)}{\bar{\rho}_{\text{HI}}(z)} u_{\text{HI}}(\ell | M, z).$$

(2D HI temperature fluctuation field)

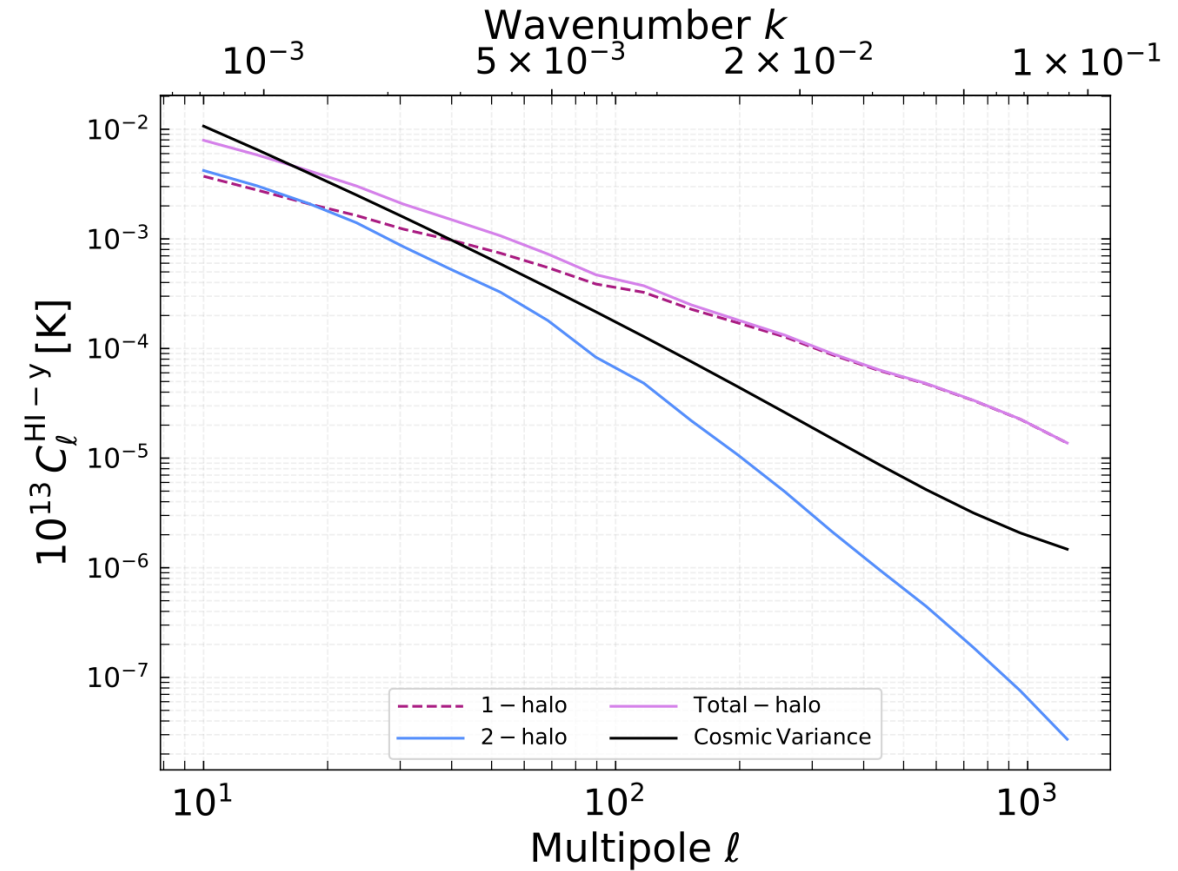
$$C_\ell^{\text{XY}, 1\text{h}} = \int_{z_{\min}}^{z_{\max}} dz \frac{c\chi^2(z)}{H(z)} G_\ell^{\text{XY}}(z)$$

$$G_\ell^{\text{XY}}(z) = \int_{M_{\min}}^{M_{\max}} dM \frac{dn}{dM}(M, z) X_\ell(M, z) Y_\ell(M, z)$$

$$C_\ell^{\text{XY}, 2\text{h}} = \int_{z_{\min}}^{z_{\max}} dz \frac{c\chi^2(z)}{H(z)} P_m^{\text{lin}}(k, z) b_\ell^{\text{X}}(z) b_\ell^{\text{Y}}(z)$$

$$b_\ell^{\text{Y}}(z) = \int_{M_{\min}}^{M_{\max}} dM \frac{dn}{dM}(M, z) b(M, z) Y_\ell(M, z)$$

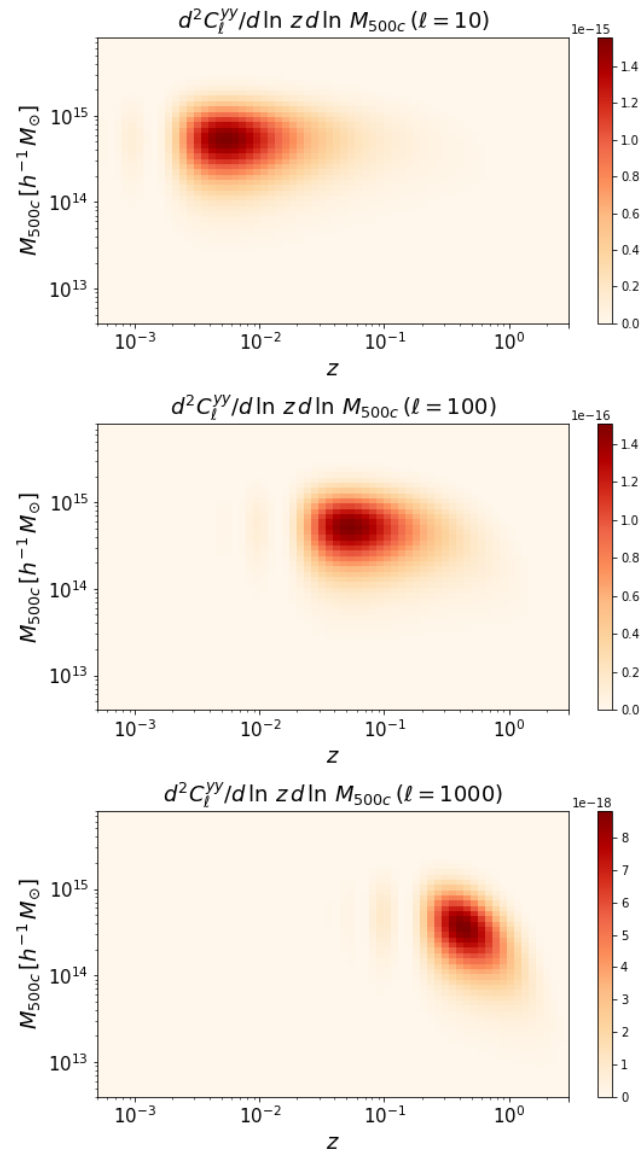
Fisher Forecast



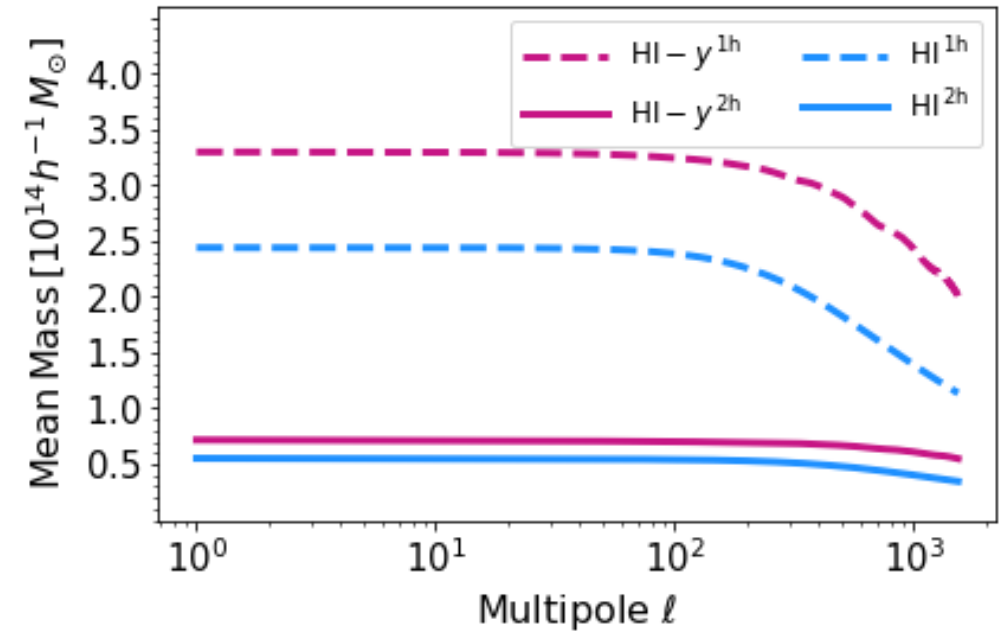
At $\ell \leq 1500$, the massive halos with more HI could also have a stronger tSZ effect.

Beyond this ($\ell \geq 30000$ or $k \geq 2h/\text{Mpc}$), HI distribution must be discrete and considered carefully.

Redshift Dependence

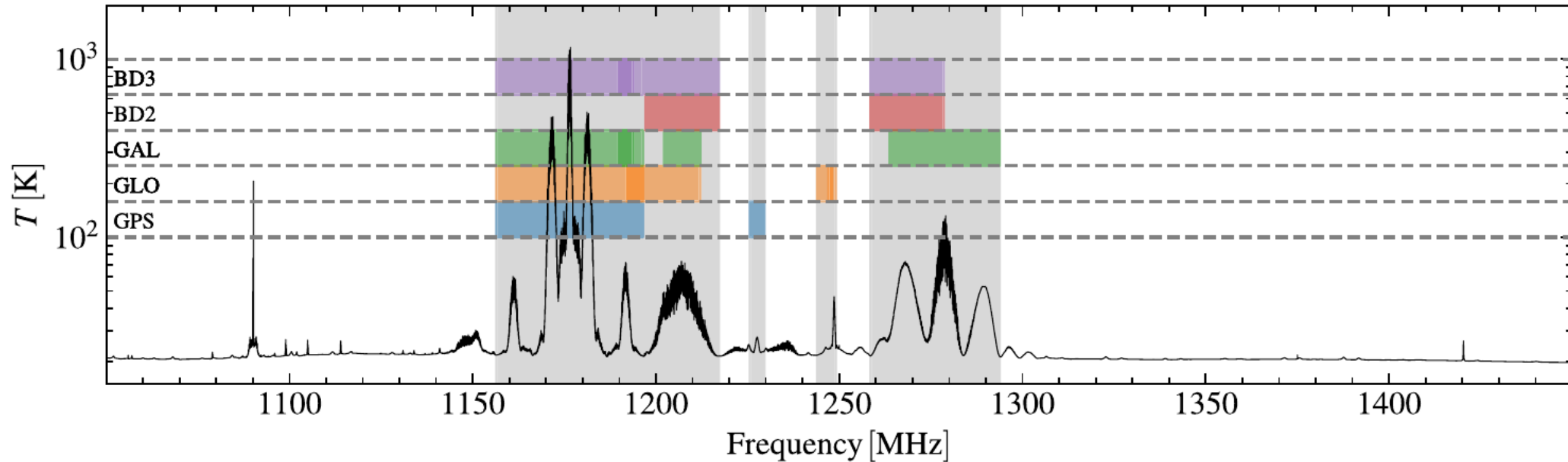


Mass Dependence



RFI dominated frequency range.

$0.09 < z \leq 0.235$



Noise

- ❖ Thermal noise for FAST is modeled as a Gaussian white noise (**Wilson et. al 2013**)
- ❖ Planck data has a Std map
- ❖ Thermal noise vs cosmic variance (**Padmanabhann et. al 2020, Lin et.al 2012**)

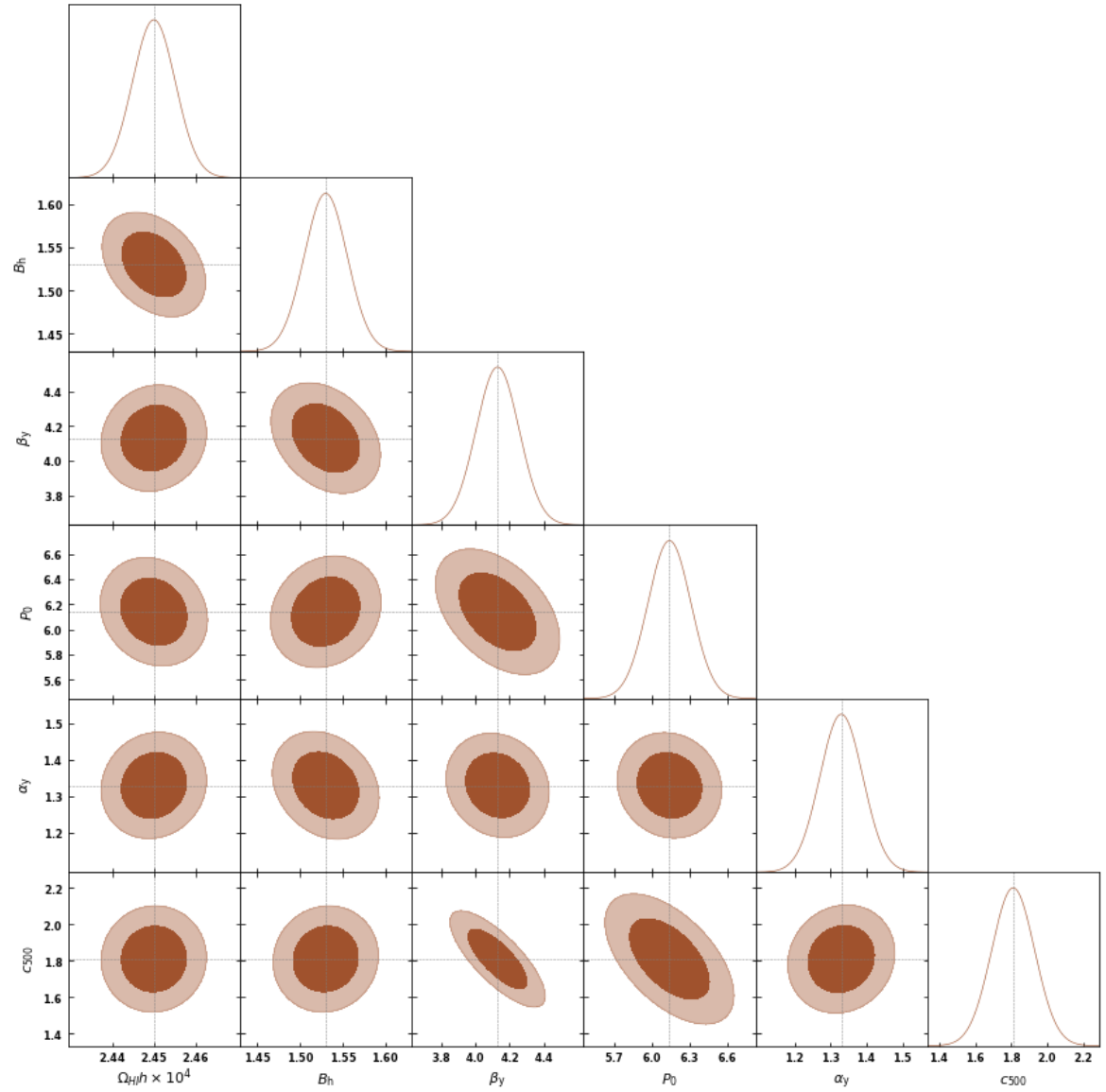
$$N_{\ell}^{XY} = \frac{\delta_{\ell\ell}}{f_{\text{sky}}^{XY} (2\ell + 1) \Delta\ell} \left[\hat{C}_{\ell}^X \hat{C}_{\ell}^Y + \hat{C}_{\ell}^{XY} \hat{C}_{\ell}^{XY} \right]$$

Foreground

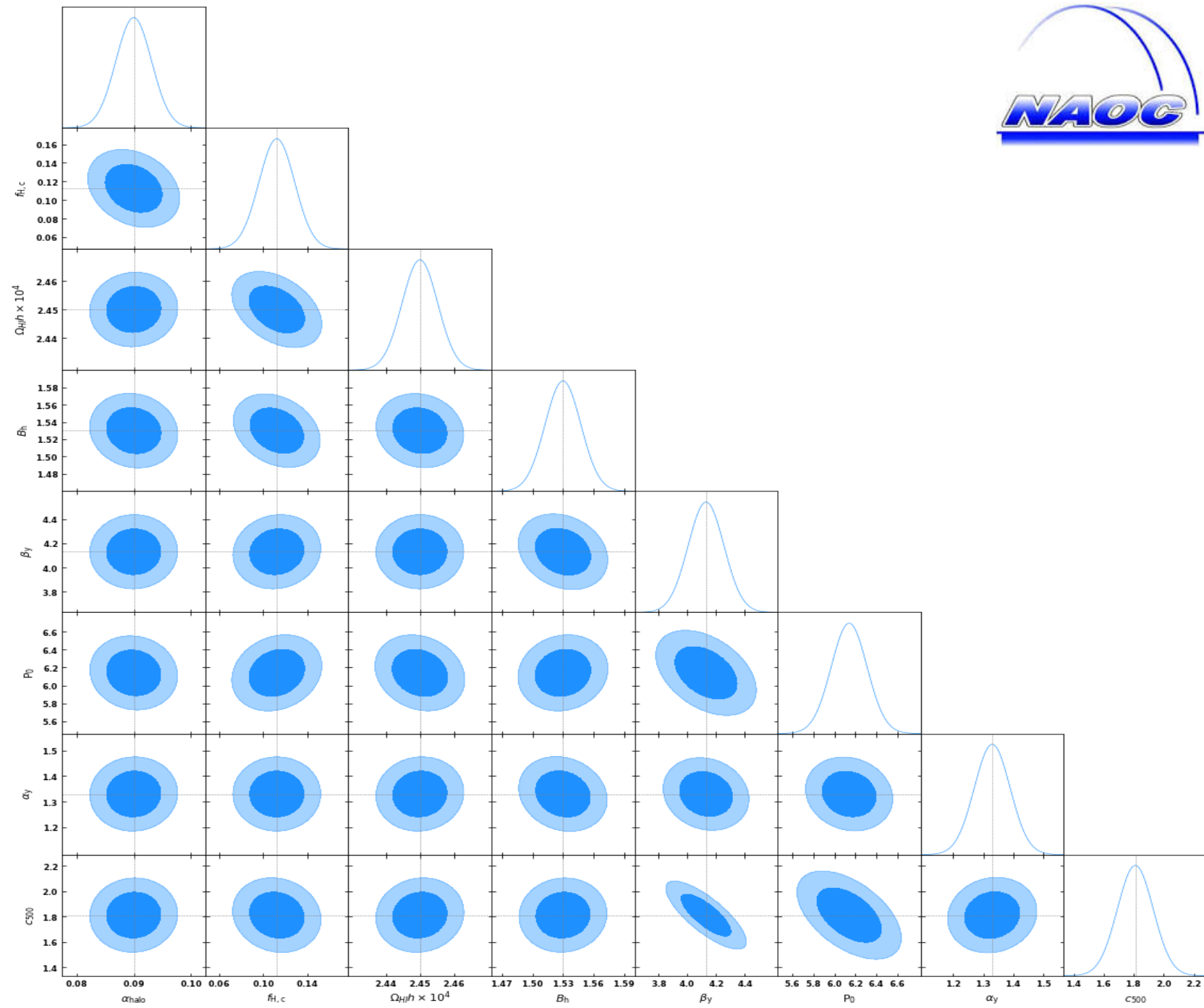
- ❖ 21 cm x CMB lensing is more robust against the foreground and other systematics than the auto-correlation of 21cm (**Dash & Guha Sarkar 2021**)
- ❖ largest scales at $\ell \leq 5$ suffers from effective foreground cleaning (**Witzemann et al 2019, Cunningtom et al. 2019**)
- ❖ Foregrounds due to the Milky way emissions are uncorrelated with the tSZ Compton-y field.

Improved constraints on Ω_{HI}

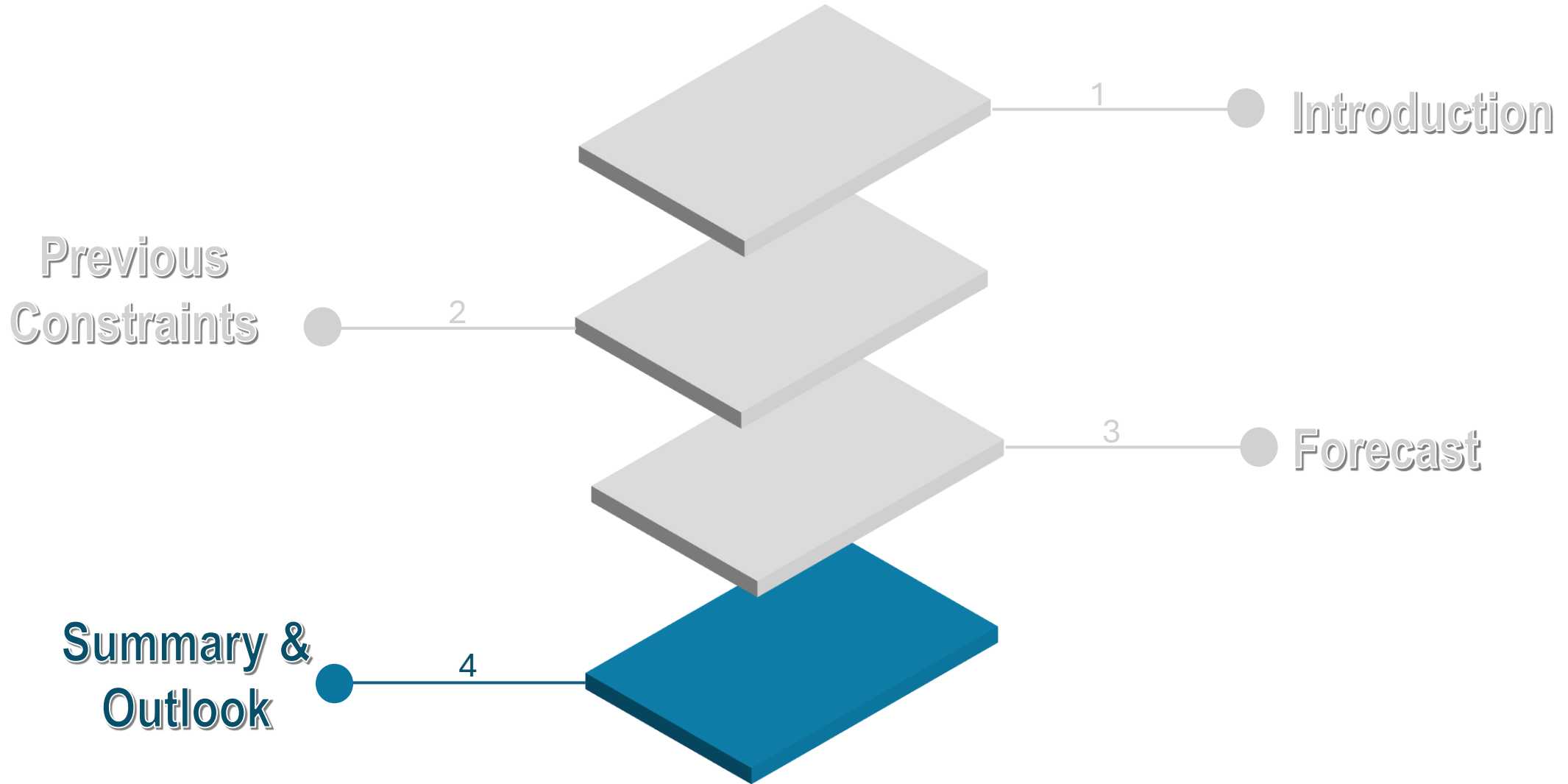
$$F_{ab} = \sum_{\ell_{\min}}^{\ell_{\max}} \frac{1}{2} \text{tr}[C_{\ell,a} \Sigma_{\ell} C_{\ell,b} \Sigma_{\ell}]$$



Constraints on M_{HI} parameters



OUTLINE



Summary & Outlook

- ❖ Analysis that incorporates tests for possible systematics such as those arising from the survey area effect, foreground effect, RFI flagging, and noise effect would likely lead to more accurate cosmological constraints from the HI-tSZ angular power spectrum.
- ❖ Would HI²-tSZ analysis using simulation be needed to test correlation at small scales?
- ❖ This constraint appears smaller than the previous estimate on the error of the HI cosmic density because we have assumed a larger sky coverage $\sim 20,000\text{deg}^2$ and longer integration time.



THANKS
FOR
LISTENING